Mat. Res. Soc. Symp. Vol. 635 © 2001 Materials Research Society

Nanosphere Lithography: Synthesis and Application of Nanoparticles with Inherently Anisotropic Structures and Surface Chemistry

Christy L. Haynes, Amanda J. Haes, and Richard P. Van Duyne
Department of Chemistry, Northwestern University
Evanston, IL 60208-3113, U.S.A.

ABSTRACT

Early work with size-tunable periodic particle arrays (PPAs) fabricated by nanosphere lithography (NSL) demonstrated that the localized surface plasmon resonance (LSPR) could be tuned throughout the visible region of the spectrum. The LSPR is sensitive to changes in nanoparticle aspect ratio and local dielectric environment. This property has recently been exploited to develop a novel method of measuring surface-enhanced Raman scattering (SERS) excitation profiles. Single layer PPAs consist of size-tunable anisotropic nanoparticles that can be modified to exhibit anisotropic surface chemistry. This work demonstrates multiple schemes for PPA modification using self-assembled monolayers and colloid decoration. Nanoparticle anisotropy can be further exploited with the recent combination of NSL and reactive ion etching (RIE); this extends the two-dimensional PPA structure into the third dimension

INTRODUCTION

In recent years, it has become possible to investigate the size dependent nature of chemical and physical properties in the nanoscale regime. While "top-down" nanoarchitecture techniques are the natural extension from previous capabilities, "bottom-up" approaches are gaining popularity.[1] This paper discusses the application of the "bottom-up" nanofabrication strategy nanosphere lithography (NSL) to create structurally anisotropic nanoparticles. Deckman et al pioneered the NSL technique wherein the natural self assembly of a monolayer of nanospheres forms a hexagonally close-packed crystal.[2] Deposition of material through this colloidal crystal mask, with subsequent removal of the nanospheres, results in an array of evenly spaced, homogeneous nanoparticles known as a periodic particle array (PPA) (Figure 1).[3] The dimension of these truncated tetrahedral nanoparticles can be tuned by choice of nanosphere diameter and deposition thickness (b). While it is possible to study the behavior of any chemical

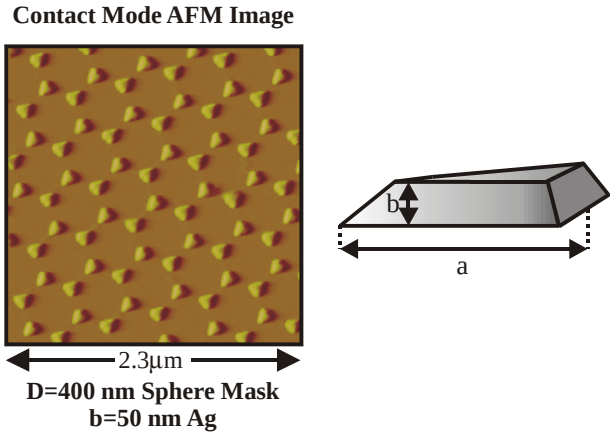

Figure 1. *AFM image of Ag PPA and graphical illustration of a single nanoparticle.*

or physical property as a function of material size regime, the optical properties of metallic nanoparticles hold special significance in the field of surface-enhanced Raman scattering (SERS), and thus, are the focus of this work.

SERS was first witnessed in 1974 by Fleishmann et al.[4] However, the true significance of the amplified Raman signals was not understood until 1977 when Jeanmaire and Van Duyne attributed the large signals to an electromagnetic enhancement.[5] Until recently, most experimental work in SERS was devoted to determining how the 10^6 SERS enhancement is divided between the chemical (CHEM) and the electromagnetic (EM) enhancement mechanisms. The CHEM is based on the concept of site-specific adsorption and is therefore a short-range effect.[6] While the CHEM enhancement mechanism is important, the EM enhancement mechanism contributes the majority of the total SERS enhancement. The EM enhancement mechanism is based on the concept that electrons in a roughened metal surface will oscillate collectively when the plasma of electrons is excited by an incoming photon of a characteristic frequency. The collective oscillation has two consequences: 1) the resonant photons are selectively absorbed and 2) electromagnetic fields are generated around the nanoparticle roughness feature. This collective electron oscillation is known as the localized surface plasmon resonance (LSPR) and is easily monitored by standard UV-vis absorption spectroscopy. When a Raman active molecule is positioned within the generated electromagnetic fields, the Raman signal increases by up to eight orders of magnitude.[7] Both chemical and conformational information can be elucidated from SERS data, but because the enhancement mechanisms are not fully understood, it is difficult to optimize SERS experiments.

In effort to understand the fundamental principles of SERS, the size dependence of the LSPR has been investigated. Previous attempts to optimize SERS experiments utilize a technique known as a wavelength-scanned excitation profiles.[8] In these experiments, one roughened metal substrate is dosed with a non-resonant Raman-active molecule, and Raman spectra are captured with multiple excitation wavelengths. This technique is undesirable because the experiment is limited by the number of available irradiation wavelengths and the changing Raman bands. By combining LSPR control with the topographic, optical, and spectroscopic measurements, a more flexible approach for excitation profiling is possible.

Intensive study has shown that nanoparticle optical properties depend on nanoparticle material, size, shape, substrate, and dielectric environment. Recent extensions of NSL explore nanoparticle templating to create anisotropic surface chemistry and embedding of the nanoparticles into the substrate material.

EXPERIMENTAL DETAILS

Materials. Ag (99.99%, 0.50 mm diameter) was purchased from D. F. Goldsmith (Evanston, IL). Borosilicate glass substrates were Fisher brand No. 2 cover slips from Fisher Scientific. Tungsten vapor deposition boats were acquired from R. D. Mathis (Long Beach, CA). Polystyrene nanospheres of various diameters were purchased from Interfacial Dynamics Corporation (Portland, OR). 1-Hexanedithiol (1-HDT) and trans-1,2-bis(4-pyridyl)ethylene were purchased from Aldrich Chemical Company (Milwaukee, WI). Silver and gold colloid solutions were prepared according the preparation by Lee and Meisel.[9] For all steps of substrate preparation, water purified with cartridges from Millipore (Marlborough, MA) to a resistivity of 18 MΩ was used.

Substrate Preparation. Glass substrates were cleaned by immersion in 3:1 concentrated H_2SO_4:30% H_2O_2 at 80°C for one hour. After cooling, the substrates were rinsed repeatedly with millipure water and then sonicated for 60 minutes in 5:1:1 H_2O:NH_4OH:30%H_2O_2 solution. Following sonication, the substrates were again rinsed repeatedly with water and then used immediately or stored in water for no longer than one week.

Periodic Particle Array Preparation. Single-layer periodic particle arrays (SL PPAs) were prepared using NSL. Nanospheres used to form deposition masks on glass substrates were used as received without any further dilution with a surfactant solution. Once the 2D colloidal crystal deposition mask was formed, the substrates were mounted into the chamber of a Consolidated Vacuum Corporation vapor deposition system. Ag films of various thicknesses were then deposited over the nanosphere mask. The mass thickness for each film was measured using a Leybold Inficon XTM/2 deposition monitor quartz crystal microbalance (East Syracuse, NY). After the Ag deposition, the nanosphere mask was removed by sonicating the entire substrate in either CH_2Cl_2 or absolute ethanol for 2 minutes. An array of nanoparticles with P_{6mm} symmetry remains on the substrate. In general, domain sizes of 35 μm^2 are achieved with low defect density. The negligible effect of defect sites has been previously addressed.[10]

AFM and UV-vis Extinction Spectroscopy Measurements. AFM images were collected under ambient conditions using a Digital Instruments Nanoscope III microscope operating in either contact mode or tapping mode. Etched Si nanoprobe tips (Digital Instruments, Santa Barbara, CA) with spring constants of approximately 0.15 N m^{-1} were used. These conical shaped tips had a cone angle of 20° and an effective radius of curvature of 10 nm. The resonance frequency of the Tapping mode cantilevers was measured to be between 280-330 KHz. The AFM images presented here represent raw, unfiltered data. Extinction spectra were recorded in standard transmission geometry using an Ocean Optics SD2000.

SERS Measurements. The probe laser was the 514.5 nm output of the Spectra-Physics Beamlok 2060 Ar^+ laser. The light was sent through a holographic notch plus filter (Kaiser Optical Systems, Ann Arbor, MI) that eliminates the reflected laser light and the Rayleigh scattered light. The laser spot size, approximately 2 μm in diameter, is much smaller than the typical PPA domain size. The remainder of the light was focused with a 43X objective into a 200 μm core diameter multi-mode optical fiber (Ensign-Bickford, Simsbury, CT) that carried the light to the spectrometer. Light exiting this fiber was collimated with a home-built expanding 4X telescope. The collimated light was then focused into the entrance of a single grating 0.5 meter monochromator (VM-505, Acton, Acton, MA) and measured with a LN_2-cooled CCD detector (PM-512, Photometrics, Tucson, AZ).

RIE Apparatus. The 2D colloidal crystal deposition masks were mounted into the chamber of a home-built RIE chamber. The substrate was then etched with 20 mTorr CF_4 at 2.2 W/cm^2 for varied lengths of time.

DISCUSSION

Anisotropic Structure – SERS Excitation Profiles. The location of the LSPR is dependent on the size, shape, and dielectric environment of the sample. Independent control of each of these factors allows tunablility of the LSPR to any wavelength in the visible, near infrared, or mid infrared regions of the spectrum.[11] With this capability realized, the opportunity exists to correlate structural, optical, and spectroscopic data in order to better understand the SERS phenomena. In this investigation, the power of these tunable, anisotropic

nanoparticles is exploited in an innovative new method to probe the SERS excitation profile in a way that is significantly simpler to implement experimentally than the traditional excitation wavelength-scanned approach. Control of particle shape and size allows use of this novel height-scanned excitation profile rather than the standard wavelength-tuned excitation profile, allowing optimization of the SERS enhancement by tuning the particle geometry and laser excitation wavelength.

The general method for performing a height-scanned excitation profile has three steps: 1) fabricate several PPA samples, maintaining equivalent structural parameters with the exception of deposition height, 2) adsorb the Raman active molecule and measure the LSPR by UV-vis extinction spectroscopy, and 3) measure the SERS spectrum from each sample with the same Raman excitation wavelength (λ_{ex}). A plot of the LSPR versus the SERS intensity of any vibrational band will show the correlation between the roughened metal surface's physical characteristics and the resulting SERS enhancement.

A sample data set with six PPA samples is shown in Figure 2. Silver PPAs were fabricated on glass with in-plane widths of approximately 80 nm and out-of-plane heights ranging from 13 nm to 63 nm. Each sample was incubated in a 5 mM solution of *trans*-1,2-bis(4-pyridyl)ethylene (BPE) before extinction spectra were measured. The LSPR wavelengths of these samples ranged from 519 nm to 707 nm. While the pyridine aromatic ring stretch (1608 cm^{-1}) and the trans alkene stretch (1640 cm^{-1}) peaks were discernable in all six λ_{ex}=514.5 nm spectra, the intensity differences were vast. The maximum signal measured for the 1640 cm^{-1} peak was almost two orders of magnitude larger than the minimum signal. When plotting the wavelength of the LSPR versus the Raman intensity of the 1640 cm^{-1} peak, the resulting curve shows a maximum at 535 nm, red-shifted 20 nm from the excitation wavelength (Figure 2).

Anisotropic Surface Chemistry. While exploring the size dependent properties of PPAs, a myriad of novel nanostructures have been developed. Two classes of nanostructures with anisotropic surface chemistry have been among those generated: 1) nanoparticle templates and 2) nanowells.

One extension of the basic NSL technique utilizes the standard noble metal SL PPA as a template for molecular patterning. In a proof-of-concept experiment, a Ag SL PPA was used as a template for dithiol molecules. Metal colloids were then bound to the free end of the dithiol molecule to prove templating capability quantitatively by AFM. By modifying the order of

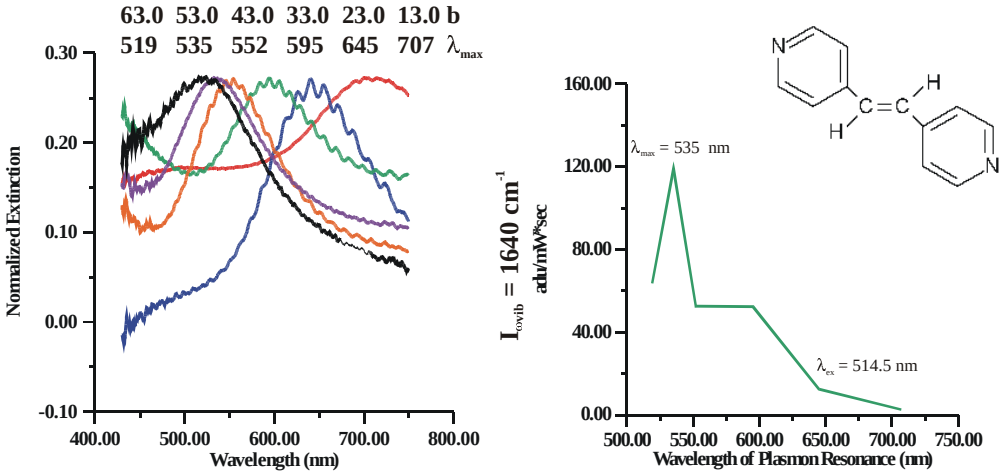

Figure 2. *Extinction spectra and height-scanned excitation profile for trans-alkene stretch of BPE of Ag PPA surface.*

nanosphere mask removal and dithiol dosing, it is possible to deposit dithiol molecules only on the top face of the nanoparticles or to surround the nanoparticles on four sides by dithiol molecules. In both decoration schemes, one must first self-assemble the colloidal crystal mask and deposit gold or silver through the mask holes. In order to deposit colloidal particles only on the top face of the nanoparticles, incubation in the dithiol solution must occur before removing the sphere mask. In this case, the linker molecule will only bind on the top of the nanoparticles, and soaking the sample in gold or silver colloid solution yields a PPA with colloids bound only to the top surface of the nanoparticles (Figure 3B). If fully colloid-coated nanoparticles are desired, the sphere mask must be removed before soaking the PPA sample in the dithiol solution. Because linker molecules can access the entire nanoparticle, colloids will surround the nanoparticles as well (Figure 3C).

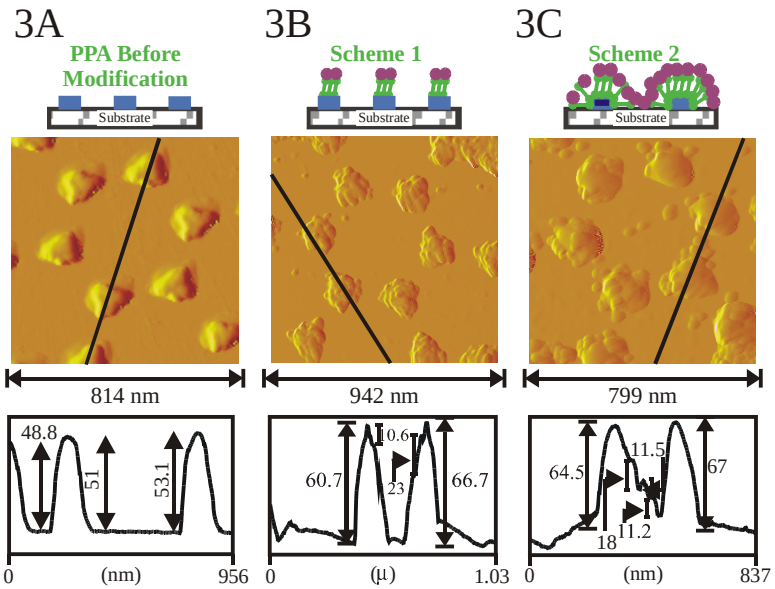

Figure 3. *Ag single layer PPAs as templates for colloidal patterning*

Anisotropic labeling of the template nanoparticles is possible with this NSL technique. AFM evidence proves that the molecular diffusion through the nanosphere mask is directional. Consequently, it should be possible to label the top and the sides of the template nanoparticle with different molecules. Surface-enhanced spectroscopic studies of these bifunctionalized nanoparticles will yield information about enhancement as a function of topography.

The second new nanoarchitecture promoting anisotropic surface chemistry implements the polystyrene nanosphere mask as a reactive ion etching (RIE) mask. When CF_4 plasma strikes the polystyrene nanospheres, the hydrocarbons are fluorinated. This non-volatile product is not etched away, so the spheres act as an etch stop. Meanwhile, as the CF_4 plasma penetrates the holes in the sphere mask, volatile SiF_2 radicals and SiF_x products are etched away.[12] The resulting structures are PPA-shaped nanowells.

Deposition of material through the nanosphere mask after etching embeds nanoparticles within the substrate. The LSPR has been measured from silver nanoparticles embedded in Si(111) and SiO_2 substrates. Future studies will explore applications of nanowell, nanorod, layered nanoparticles in nanowell, and fully embedded nanoparticle systems.

CONCLUSION

The presented excitation profile results clearly demonstrate the power of understanding the role of the LSPR in the SERS enhancement mechanism, and this work would not be possible without the predictable, tunable anisotropic nanoparticles fabricated with the NSL technique. The most important consequence of this work is that there is a SERS-active substrate that is fully characterized. Future correlation of experimental results with electrodynamic modeling[10] will advance the goal of understanding the relationship between the surface topography, the location of the LSPR, and the enhancement mechanism of SERS

The extension of NSL to the fabrication of nanoparticles with anisotropic surface chemistry holds much future promise. The ability to selectively label varying nanoparticle faces will contribute to sensing and barcoding applications. The powerful combination of NSL and RIE not only presents nanoparticles with anisotropic dielectric environments, but also suggests that very high aspect ratio nanoparticles can be fabricated by this flexible synthesis technique.

ACKNOWLEDGEMENTS

The authors would like to acknowledge Michelle Duval Malinsky for her work on the nanoparticle templating project and Dr. John Ketterson for the use of the RIE chamber and helpful discussions. This research was supported by the MURI ARO (Grant DAAG55-97-1-0133), NSF (Grant CHE-940078), and MRSEC program of the NSF (Grant DMR-0076097).

REFERENCES

1. M. B. Mohamed, K. Z. Ismail, S. Link, M. A. El-Sayed, *Journal of Physical Chemistry B.*, **102**, 9370-9374 (1998).
2. H. W. Deckman, J. H. Dunsmuir, *Applied Physics Letters*, **41**, 377-379 (1982).
3. J. C. Hulteen, R. P. Van Duyne, *Journal of Vacuum Science and Technology A*, **13**, 1553-1558 (1995).
4. M. Fleischmann, P. J. Hendra, A. J. McQuillan, *Chemical Physics Letters*, **26**, 163-166 (1974).
5. D. L. Jeanmaire, R. P. Van Duyne, *Journal of Electroanalytical Chemistry*, **84**, 1-20 (1977).
6. M. Moskovits, *Reviews of Modern Physics*, **57**, 783-826 (1985).
7. G. C. Schatz, The Image Field Effect: How Important Is It?, *Surface Enhanced Raman Scattering*, eds. R. K. Chang, T. E. Furtak (Plenum Press, 1982) pp. 35-50.
8. P. F. Liao, J. G. Bergman, D. S. Chemla, A. Wokaun, J. Melngailis, A. M. Hawryluk, N. P. Economou, *Chemical Physics Letters*, **81**, 355-359 (1981).
9. P. C. Lee, D. Meisel, *Journal of Physical Chemistry*, **86**, 3391-3395 (1982).
10. T. R. Jensen, M. L. Duval, L. Kelly, A. Lazarides, G. C. Schatz, R. P. Van Duyne, *Journal of Physical Chemistry B*, **103**, 9846-9853 (1999).
11. T. R. Jensen, M. D. Malinksy, C. L. Haynes, R. P. Van Duyne, *Journal of Physical Chemistry B*, **104**, 10549-10556 (2000).
12. G. Cunge, P. Chabert, J. Booth, *Plasma Sources Science and Technology*, **6**, 349-360 (1997).